Mode of Action of the Catalytic Site in the N-Terminal Ribosome-Inactivating Domain of JIP60[1]

Michal Przydacz, Rhian Jones,[2] Helen G. Pennington, Gerard Belmans, Maya Bruderer,[3] Rachel Greenhill,[4] Tia Salter,[5] Peter A.D. Wellham, Ernesto Cota, and Pietro D. Spanu[6,7]

Department of Life Sciences, Imperial College London, London SW7 2AZ, United Kingdom

ORCID IDs: 0000-0002-2980-9079 (H.G.P.); 0000-0003-4816-1148 (R.G.); 0000-0001-9571-4038 (T.S.); 0000-0003-2725-4513 (P.A.D.W.); 0000-0001-8928-6049 (P.D.S.).

Jasmonate-induced protein 60 (JIP60) is a ribosome-inactivating protein (RIP) from barley (*Hordeum vulgare*) and is involved in the plant immune response dependent on jasmonate hormones. Here, we demonstrate in *Nicotiana benthamiana* that transient expression of the N-terminal domain of JIP60, from which the inhibitor domain (amino acids 163–185) is removed, initiates cell death, leading to extensive necrosis of leaf tissues. We used structure prediction of JIP60 to identify potential catalytic amino acids in the active site and tested these by mutagenesis and in planta assays of necrosis induction by expression in *N. benthamiana*, as well as through an in vitro translation-inactivation assay. We found that Tyr 96, Glu 201, Arg 204, and Trp 234 in the presumptive active site of JIP60 are conserved in 815 plant RIPs in the Pfam database that were identified by HUMMR as containing a RIP domain. When these amino acid residues are individually mutated, the necrosis-inducing activity is completely abolished. We therefore propose that the role of these amino acids in JIP60 activity is to depurinate adenosine in ribosomes. This study provides insight into the catalytic mechanism of JIP60.

Jasmonates (JAs) are an important group of phytohormones associated with immune responses in plants (Wasternack and Hause, 2013). Immunity triggered by pathogen-associated molecular patterns leads to accumulation of JAs. JAs are potent hormones involved in reprogramming the plant toward defense against pathogens and they are sufficient to induce the hypersensitive response in grapevine (*Vitis vinifera*) in the absence of pathogens (Repka et al., 2001). JAs also promote processes leading to senescence in barley (*Hordeum vulgare*; Bachmann et al., 2002).

The actual bioactive jasmonate is a +(7)-iso-JA-Ile conjugate (Staswick and Tiryaki, 2004; Fonseca et al., 2009; Wasternack and Hause, 2013; Chini et al., 2016), and JA-mediated responses are promoted by the perception of JA-Ile by the coronatine insensitive1 protein (COI1-JAZ) coreceptor that triggers the signaling pathway. JAs induce a broad range of proteins, including JA-induced proteins (JIPs), that may be involved in plant defense (Chini et al., 2016; Goossens et al., 2016).

There is a range of currently identified JIPs, such as JIP54 and JIP24, which are an allene oxidase synthase and cyclase, respectively, and a lipoxygenase, JIP100, and all of these JIPs are part of the JA biosynthesis pathway (Vörös et al., 1998; Maucher et al., 2000, 2004; Wasternack and Feussner, 2018; Wasternack and Strnad, 2018). In cereals, JIP23 plays a role in response to abiotic stresses and down-regulation of photosynthesis (Hause et al., 1994, 1999). The highly expressed JIP37 is found in the cytoplasm, nucleus, and vacuole, but its function remains unknown (Leopold et al., 1996).

MethylJA (MeJA) is often used as a JA-Ile mimic in exogenous treatments. MeJA induces JIP15, a precursor of the thionin JIP6, a fungitoxic molecule localized in the plant cell wall and vacuole (Bohlmann et al., 1988; Andresen et al., 1992; Reinbothe et al., 1997). MeJA leads to increased resistance to *Blumeria graminis* in wheat (*Triticum* sp.), and this may work via induction of a range of pathogenesis-related proteins (Duan et al., 2014).

[1]This work was supported by the Biotechnology and Biological Sciences Research Council (BBSRC; grant nos. BB/M000710/1 and BB/J014575/1 to P.D.S.) and the European Research Area Network for Coordinating Action in Plant Sciences (ERA-CAPS) project DURESTrit (no. PA 861/13).

[2]Present address: AFMB UMR 7257 Case 932, Campus de Luminy, 163 Avenue de Luminy, 13288 Marseille CEDEX 09.

[3]Present address: Biozentrum, University of Basel, Klingelbergstrasse 70, 4056 Basel, Switzerland.

[4]Present address: Department of Animal and Plant Sciences, University of Sheffield, Western Bank, Sheffield, S10 2TN, United Kingdom.

[5]Present address: School of Biochemistry, Biomedical Sciences Building, University Walk, Bristol BS8 1TD, University of Bristol, United Kingdom.

[6]Author for contact: p.spanu@imperial.ac.uk.

[7]Senior author.

The author responsible for distribution of materials integral to the findings presented in this article in accordance with the policy described in the Instructions for Authors (www.plantphysiol.org) is: Pietro D. Spanu (p.spanu@imperial.ac.uk).

M.P. modelled the protein structure, established the in planta expression model, analyzed the results and wrote the first draft of the manuscript; R.G. and M.B. created and tested the isofunctional and isostructural JIP60ml mutants; R.J. and H.P. cloned and created the recombinant JIP60ml; P.W. analyzed the bioinformatics of the predicted JIP60ml active site; G.B. and T.S. carried out the in vitro assays; E.C. supervised the structural analysis; P.D.S. conceived the project, supervised the experimental work, and revised the manuscript with contributions from all other authors.

www.plantphysiol.org/cgi/doi/10.1104/pp.19.01029

One of the best known JIPs in barley is JIP60 (Chaudhry et al., 1994). JIP60 is a complex protein with an N-terminal domain that acts as a ribosome-inactivating protein (RIP) and a C-terminal domain that resembles a eukaryotic initiation factor IV (Reinbothe et al., 1994; Wasternack and Hause, 2013). RIPs have been studied for a long time. The most studied RIP by far is ricin, derived from castor bean (*Ricinus communis*), which is often used as a model RIP. The first identification of ricin and abrin, and their description as proteins by Paul Ehrlich, dates back to the late 19th century (Bolognesi et al., 2016). The interest in RIPs was rekindled by the demonstration that their cytotoxic properties make them potential antitumor agents (Lin et al., 1970). It was suggested that they could be used clinically as immunotoxins by conjugation with targeted antibodies (Pastan et al., 1992).

RIPs are proposed to act as N-glycosidases. Ribosome inactivation is achieved by depurination of a ubiquitously conserved adenine within a GAGA motif on the large ribosomal subunit RNA (Schrot et al., 2015). The target adenine of the GAGA motif is located on a part of ribosomal RNA (rRNA) often referred to as the α-sarcin/ricin loop (Endo and Tsurugi, 1987; Stirpe et al., 1992; Dunaeva et al., 1999). The RIP-mediated depurination of the adenine prevents elongation factors from binding to the ribosome and arrests the translation at the elongation step (Lancaster et al., 2008). This leads to irreversible ribosome degradation, protein translation inhibition, and subsequent cell death (Narayanan et al., 2005). Although RIPs predominantly target the α-sarcin/ricin loop, they are often capable of depurination of several other sites on a ribosome (Barbieri et al., 1992).

In plants, RIPs may have distinct functions, as reflected by differential patterns of expression. For example, barley RIP30 is expressed in the seed germ but not in the mature plant, whereas JIP60 is found in mature plants (Leah et al., 1991).

A role has been proposed for RIPs in plant defense. For instance, the pokeweed (*Phytolacca americana*) antiviral protein confers both antiviral and antifungal resistance in transgenic plants (Hudak et al., 1999; Krivdova et al., 2014; Di and Tumer, 2015). Their ability to interact and cleave RNA can be used by plants to defend themselves from viral infection by cleaving viral RNA (Krivdova et al., 2014). In addition, some plants deploy RIPs as antifungal agents. For instance, overexpression of barley RIP30 in wheat leads to increased protection against *B. graminis* infection (Bieri et al., 2003). In principle, there are different ways that RIPs can act against infecting fungi: they could either be secreted and work directly as antifungal proteins or they could lead to host cell death, collapsing the infected plant cells, thus preventing the infection from spreading by nutrient deprivation (Vigers et al., 1991; Stirpe, 2013).

Three types of RIPs have been recognized. Type I RIPs (synonym type A) consist solely of a single-chain peptide with N-glycosidase activity, e.g. RIP30 from barley or tritin from wheat (Schrot et al., 2015). Type II RIPs (synonym type AB) have two distinct domains: the N-terminal N-glycosidase is responsible for ribosome inactivation, and the C-terminal lectin domain is necessary for transmembrane trafficking. The prime example of type II RIPs is ricin. The rare type III RIPs, such as JIP60, are different from Types I and II. JIP60 possesses two distinct domains but the B domain is not a lectin. Its N-terminal domain is an N-glycosidase which contains the tell-tale 17-amino acid shigatoxin motif of a RIP, whereas its C-terminal domain resembles eukaryotic initiation factor IV, the function of which is currently unknown (Chaudhry et al., 1994). To be activated, the N-terminal RIP domain requires proteolytic cleavage of a short internal peptide (an "inactivation loop"; Reinbothe et al., 1994). This is a feature shared with maize (*Zea mays*) RIP1 (De Zaeytijd and Van Damme, 2017). The inactivation loop may play a crucial role in controlling their activity in the plant (Chaudhry et al., 1994; Nielsen and Boston, 2001; Stirpe, 2013).

Barley has two paralogous genes encoding JIP60 and JIP60-like. The two genes are located in the genome close to quantitative trait loci such as powdery mildew resistance, boron sensitivity, and resistance to spot blotch (Rustgi et al., 2014). The JIP60 protein lacks a signal peptide, so it is predicted to be localized in the cytoplasm (Hause et al., 1994). When the C-terminal domain is cleaved off and the inactivation loop on the N terminus is proteolytically excised, the RIP domain becomes fully activated, leading to degradation via depurination of the α-sarcin/ricin loop and permanent ribosome inactivation (Rustgi et al., 2014).

Here, we define the basis for the biochemical action of JIP60ml, a recombinant N-terminal domain of JIP60 from which the inactivation loop was removed and replaced with a short Met Leu linker. This mimics the active form found in plants and leads to the induction of cell death when expressed in planta. To achieve this, we characterized the N-terminal domain of JIP60 (JIP60ml) using bioinformatics and in silico modeling; this led to the identification of putative key catalytic residues in the active site. Subsequently, we tested the JIP60ml ribosome-inactivating potential in planta via *Agrobacterium tumefaciens*-mediated transient expression and in vitro through transcription/translation assays and verified the importance of the catalytic amino acids by site-directed mutagenesis followed by functional assay in planta.

RESULTS

Identification of Key Residues within the JIP60 RIP Family Leads to a Proposed Mechanism of Inhibition by the Activation Loop

The amino acid sequence of the N-terminal domain of JIP60, predicted to act as a RIP, was used as a query in HMMER software (Finn et al., 2015) to find related protein sequences in the Pfam database (EMBL-European Bioinformatics Institute). The algorithm recognized the amino acid sequence as an rRNA N-glycosidase (GO: 0030590). Using the JIP60 amino acid sequence as the

query, a group of 815 sequences classified as RIPs (PF00161) were found. Interestingly, within this group, the RIP domain on average covered only 46.03% of the protein sequences, suggesting the presence of additional domains. In fact, most of the sequences appeared to belong to Type II RIPs (which have an extra domain), rather than Type I (single domain). The RIP domain family showed poor amino acid sequence conservation, with average identity of 18% in the full family alignment. However, the ClustalO (Madeira et al., 2019) alignment showed a number of residues conserved across the family (Fig. 1A), which were then highlighted using an HMM logo graph (Fig. 1B; Schuster-Böckler et al., 2004).

We hypothesized, based on their high sequence conservation, that four of these positions (Y96, E201, R204, and W234) are important for their function. To observe the structural context of these residues, we generated a homology model of JIP60ml using Phyre[2]

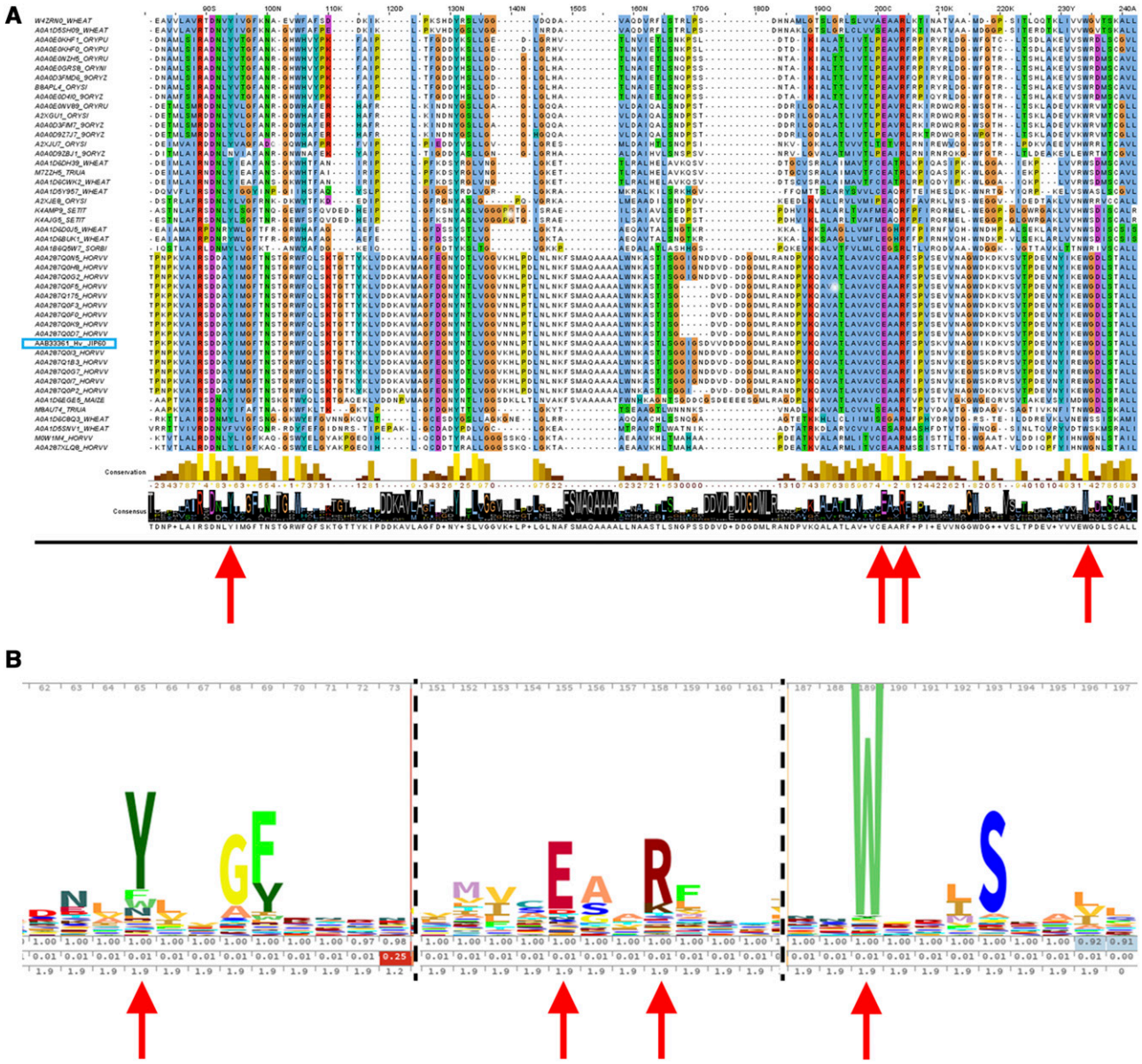

Figure 1. Alignment of amino acid sequences and hidden Markov model logo representation of the RIP domain family. A, The amino acid sequence of JIP60 RIP domain (blue rectangle) was used as the query in the Ensembl Plants database using the HMMER web tool. The sequence was recognized as a part of the RIP family (PF00161) consisting of 815 sequences. These sequences were then aligned and sorted into a neighbor-joining tree using the BLOSUM62 algorithm. This figure represents a small subset of 45 sequences most similar to JIP60. The residues are colored according to the Clustal convention. Red arrows point to residues of interest—Tyr 96, Glu 201, Arg 204, and Trp 234—on the JIP60 RIP domain. B, Logo representation using a HMM of residues conserved in the RIP domain family. The amino acid sequence of JIP60 RIP domain was used as the query for this alignment. Red arrows represent residues selected for site-directed mutagenesis.

(Kelley et al., 2015). The sequence was predicted to assume a RIP-like fold, revealing barley RIP30 (Lee et al., 2012) as the template structure with the highest sequence identity to JIP60ml (31% sequence identity from alignment of 263 residues, with 93% sequence coverage). The four conserved residues highlighted by the HMM logo clustered in the proposed catalytic site of RIP30, supporting the idea that they are key residues in the active site of JIP60ml. These four residues were selected for investigation of their involvement and nature in the ribosome-inactivating function.

The structure of the wild-type JIP60 with an inactivation loop was compared to that of the recombinant form without the inactivation loop (JIP60ml) and was also predicted using the Phyre^2 tool at the "intense" setting (100% confidence over 96% of the alignment; Fig. 2, A and B).

Predicting the Catalytic Mechanism of JIP60

Given that the active site in the N-terminal domain of JIP60 conforms to the characteristics of RIPs, it is clear that E201 and R204 may be involved in hydrolysis of the glycosidic bond between the purine and the RNA backbone, while Y96 and Y132 may act as stabilizers of the purine group in the rRNA-protein interaction. The other four residues, G98, F99, W234 and S238, show high conservation in the RIPs. G98 and F99 are buried in the structure of JIP60 and are not in close contact with E201/R204, whereas the side chain of S238 may help to orientate the side chain of W234 for a pi-cation interaction with the catalytic R204, located on the opposite side of the indole group (Fig. 2C). We propose that the catalytic mechanism of JIP60 resembles the detailed mechanism for RIPs described by Wahome et al. (2011) based on extensive studies in ricin (Fig. 3).

Expression of the Recombinant JIP60ml Domain Causes Necrosis of Plant Tissues

In order to test whether the recombinant JIP60ml is functional in planta, we expressed the recombinant protein by agroinfiltration (Lee and Yang, 2006). We created two strains of *Agrobacterium* GV3101 by transforming plasmids containing either a JIP60ml-GFP construct, or GFP only as a negative control, into the bacteria. The *Agrobacterium* cells were then introduced into *Nicotiana benthamiana* leaves by vacuum infiltration. The treated leaves were observed every day after that and photographs were taken at 2 and 7 d post-infiltration (dpi). There were no differences visible to the naked eye between the JIP60ml-treated cells and the

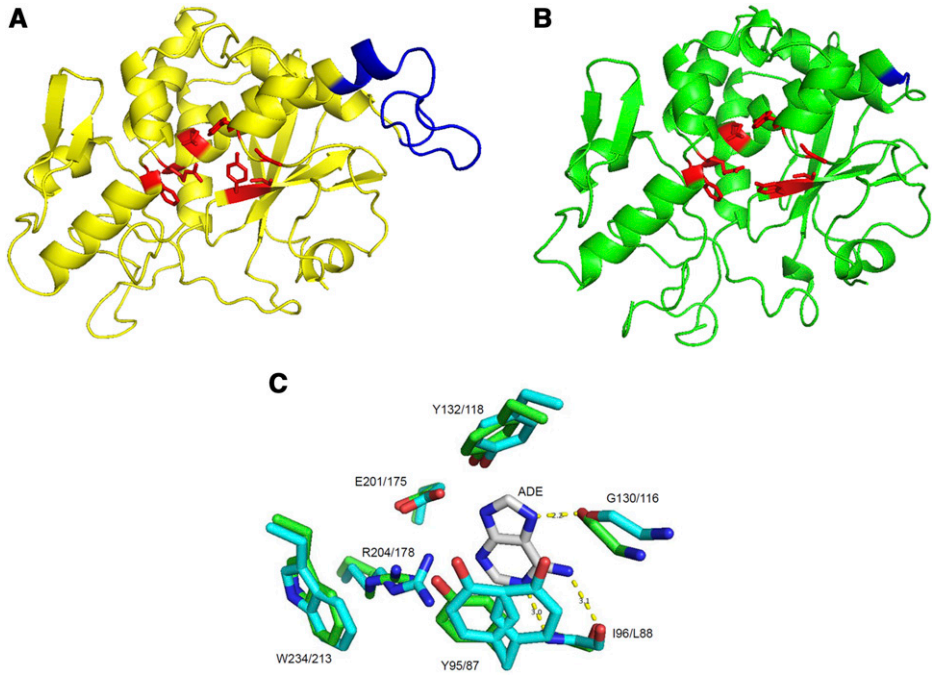

Figure 2. Predicted molecular model of the N-terminal RIP domain of JIP60. A, Model of the predicted molecular structure of the wild-type N-terminal RIP domain of barley JIP60. The blue region corresponds to the inactivation loop that needs to be excised for JIP60 to be functional. The residues colored pink represent the predicted preserved active site. B, Model of JIP60ml. The predicted N-terminal domain of JIP60 is based on sequences from which the inactivation loop was removed and replaced with a short Met-Leu linker (dark blue). The deep red residues show that the conserved amino acids we propose are key for JIP60-mediated catalysis. C, Close-up of the putative active site of the wild-type N-terminal domain of JIP60. The pink residues represent the residues that may take an active part in JIP60 function. The deep red residues represent the residues predicted to take active part in JIP60 function. All models were created using the Phyre^2 predictive algorithm on the "intense" setting.

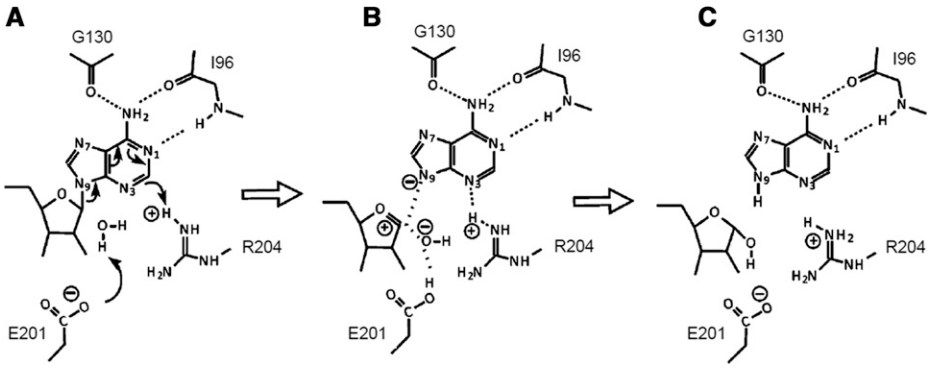

Figure 3. Proposed mode of action of hydrolytic depurination of adenine by the JIP60 RIP domain. The curved arrows represent movements of electrons, while double arrows represent temporary bonds. A, First, a negatively charged E201 leads to splitting a water molecule into H^+ and OH^-. B, Subsequently, OH^- attacks the carbon atom located on the ribose involved in a glycosidic bond with the purine. That leads to a shift of charges across purine rings, facilitated by the proximity of positively charged R204, and to a cleavage of the glycosidic bond between the ribose and purine. C, The conditions prevalent in the plant cytoplasm (pH 7.4–7.5) favor negatively charged Glu and positively charged Arg. Therefore, a reverse shift of charges takes place, which ends with a Glu-associated proton bound by the nitrogen atom located on purine. The glycosidic bond is fully cleaved and the purine is released from the adenine.

negative-control cells up to 2 dpi (Fig. 4A). However, there was an evident difference at 7 dpi (Fig. 4B); the leaf zone agroinfiltrated with JIP60ml showed clear signs of chlorosis and necrosis. The leaf lamina in that zone showed substantial thinning and proneness to tearing.

Eventually, the whole of the infiltrated area died. In contrast, the zone agroinfiltrated with the GFP-only negative control showed none of those signs. This demonstrated that recombinant JIP60ml expressed in *N. benthamiana* leaves has a severe effect. JIP60ml was extremely effective at causing necrosis, even in the nonhost plant; infiltration of *Agrobacterium* at a concentration as low as OD_{600} of 0.02 was sufficient to cause necrosis within the zone (Supplemental Fig. S1).

Predicted Active-Site Residues Are Essential for Necrosis-Inducing Activity

To test experimentally the importance of the four amino acids (Y96, E201, R204, and W234) predicted to be the catalytic site of the activated N-terminal of JIP60 (JIP60ml), the residues were individually mutated to Ala. Ala was chosen because it is a short, noninteractive amino acid unlikely to cause a structural disruption (Cunningham and Wells, 1989; Morrison and Weiss, 2001). As a control, Val 62 was chosen as a structural residue predicted not to be involved in JIP60 function, and we mutated it to an Ala as well. The mutants then were each agroinfiltrated in separate leaf zones, alongside the functional JIP60ml-GFP as a positive control and the GFP-only as a negative control (Fig. 5). The leaves were then observed daily, and pictures were taken at 3, 7, and 11 dpi. The zones agroinfiltrated with the JIP60ml positive control showed progressive degeneration of leaf tissue, as expected; in contrast, the leaf zones infiltrated with the $JIP60_{Y96A}$, $JIP60_{E201A}$, $JIP60_{R204A}$, and $JIP60_{W234A}$ mutants showed no signs of necrosis, i.e. they had lost their function. The $JIP60_{V62A}$ "control" mutant induced a necrosis that was indistinguishable from that of nonmutated JIP60ml.

Next, further investigation of the active-site residues was performed. Instead of Ala substitutions, a set of amino acids was chosen that were either isofunctional (i.e. they possessed an equivalent chemical functional group) or isostructural (i.e. they had a similar structure or size). To this end, the following mutants were created: Y96F (isostructural), Y96S (isofunctional), E201D (isofunctional), R204K (isofunctional), W234F (isostructural), and W234P (which is likely to disrupt the structure by bending the protein backbone). The purpose of these mutants was to investigate how fragile the active site is, and whether the JIP60 function can be retained with other, similar residues. These mutants were then agroinfiltrated into *N. benthamiana* leaves alongside JIP60ml

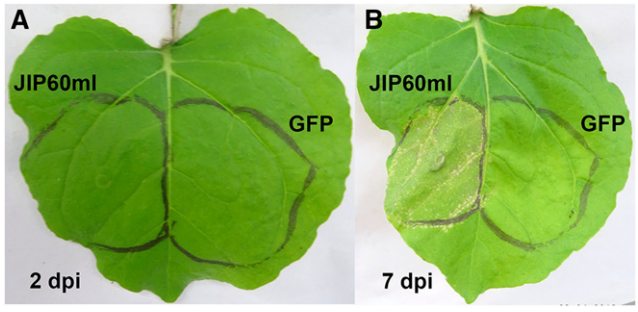

Figure 4. Transient expression of active JIP60 via agroinifiltration of *N. benthamiana*. *Agrobacterium* containing a plasmid either with JIP60ml-GFP or with GFP only as a negative control was infiltrated into *N. benthamiana* leaves (OD_{600} = 1.0). Subsequently, pictures of the leaves were taken at 2 (A) and 7 dpi (B).

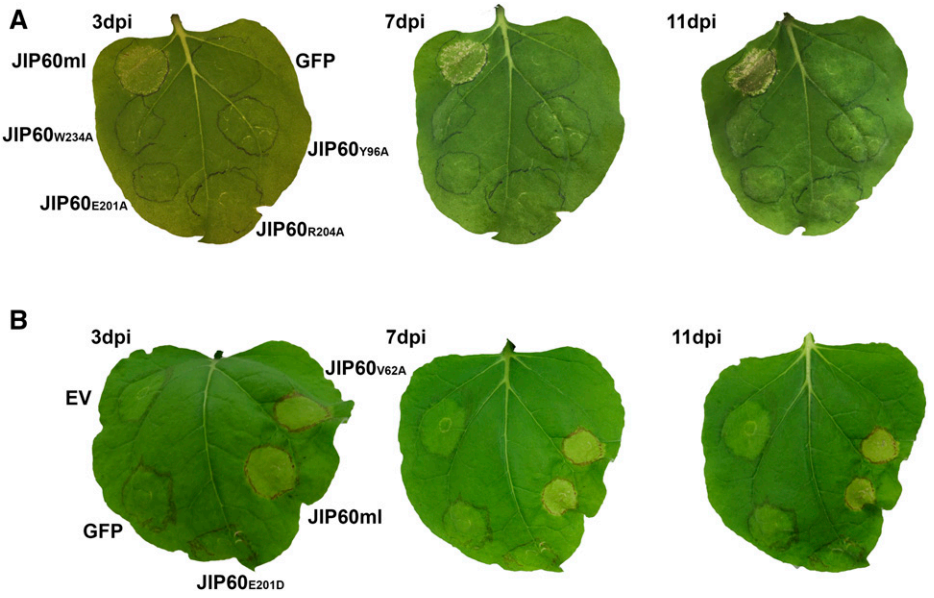

Figure 5. Time course of transient expression of JIP60 Ala substitution mutants. A, *Agrobacterium* strains containing the four JIP60 mutants ($JIP60_{Y96A}$, $JIP60_{E201A}$, $JIP60_{R204A}$, and $JIP60_{W234A}$), JIP60ml as a positive control, and GFP-only as a negative control were created. *Agrobacterium* strains were infiltrated into a *N. benthamiana* leaf as indicated (OD_{600} = 1.0) and pictures were taken at 3, 7, and 11 dpi. B, *Agrobacterium* strains containing JIP60ml, $JIP60_{V62A}$ mutants, $JIP60_{E202D}$ variants, GFP-only as a negative control, or the empty vector (EV) were infiltrated (OD_{600} = 1.0) into a *N. benthamiana* leaf as indicated, and pictures were taken at 3, 7, and 11 dpi. This experiment was repeated three times with similar outcomes.

and GFP-only as positive and negative controls, respectively. The leaves were monitored for signs of necrosis, and pictures were taken at 3, 7, and 11 dpi (Fig. 6): none of the JIP60ml mutants caused any necrosis, and all appeared the same as the GFP-only negative control. Only the leaf zones infiltrated with JIP60ml-GFP showed progressive necrosis and plant tissue degeneration, as observed previously. These results indicated that substitutions of the essential amino acids of the JIP60 active site, even with similar residues, either structurally or chemically disrupted JIP60 function.

Presence of Transiently Expressed JIP60ml Mutant Proteins In Planta

We investigated whether the absence of necrosis in the leaves agroinfiltrated with the JIP60ml mutants was the result of an actual loss of function or simply lack of protein expression. First, the agroinfiltrations were repeated and leaf discs of the infiltrated zones were collected at 2 dpi. The leaf disks were observed by epifluorescence microscopy using filters to enable the detection of fluorescence of the GFP-tagged JIP60ml mutants. A strong signal from the GFP-only control was visible in the cells of leaves at 2 dpi. The weak signal in the uninfiltrated leaf disc was considered to be background autofluorescence of the cells (Fig. 7). We observed the clear "jigsaw puzzle" outline of the GFP signal characteristic of the basal cells of the *N. benthamiana* leaf epidermis. The expression appeared uniform throughout the cytosol, and some of the fluorescence was localized in the nuclei. The micrographs of leaf discs infiltrated with JIP60ml showed no GFP signal; the very weak fluorescence observed in the micrographs is likely due to autofluorescence of compounds associated with cell death. Moreover, the cellular structure within the epithelial tissue seemed to have been compromised when compared to the uninfiltrated sample. The same results occurred in samples infiltrated with $JIP60_{V62A}$. In contrast, the majority of the loss-of-function JIP60ml variants ($JIP60_{Y96A}$, $JIP60_{Y96S}$, $JIP60_{Y96F}$, $JIP60_{E201A}$, $JIP60_{E201D}$, $JIP60_{R204A}$, $JIP60_{R204K}$, $JIP60_{W234A}$, and $JIP60_{W234P}$) exhibited strong GFP signal, indicating successful expression. Note, however, that the signal is less uniform than in the case of the GFP-only control. The GFP fluorescence in the loss-of-function JIP60ml mutants was distributed throughout the cytosol but was also evident as small puncta. Of all the JIP60ml loss-of-function variants, only $JIP60_{W234F}$ showed poor GFP signal, with only isolated cells showing any GFP expression.

We then analyzed the integrity of the recombinant proteins expressed in the agroinfiltrated plant tissues using western blotting. Leaf discs from infiltrated leaves were collected at 3 dpi. Proteins were analyzed by western blotting and probed with horseradish peroxidase (HRP)-labeled secondary antibodies. Clear HRP-positive bands were visible on the western blot; these were consistent with the 55-kD size of the JIP60ml-GFP fusion protein and were observed for all the loss-of-function JIP60ml variants except for $JIP60_{W234F}$ (Fig. 8). Those samples also showed bands corresponding to proteins of an apparent M_r of 22 kD, which we interpret to be products of protein degradation. The sample with the GFP-only control showed an intense band consistent with the recombinant GFP size of 27 kD. Samples from noninfiltrated leaf disc protein extract showed no bands. These bands were not visible in the JIP60ml and $JIP60_{W234F}$ samples.

Recombinant JIP60ml Leads to Inhibition of In Vitro Protein Translation

By definition, RIPs act primarily by inhibiting the activity of the ribosomes, i.e. translation. We therefore tested the effect of the targeted mutations on JIP60ml

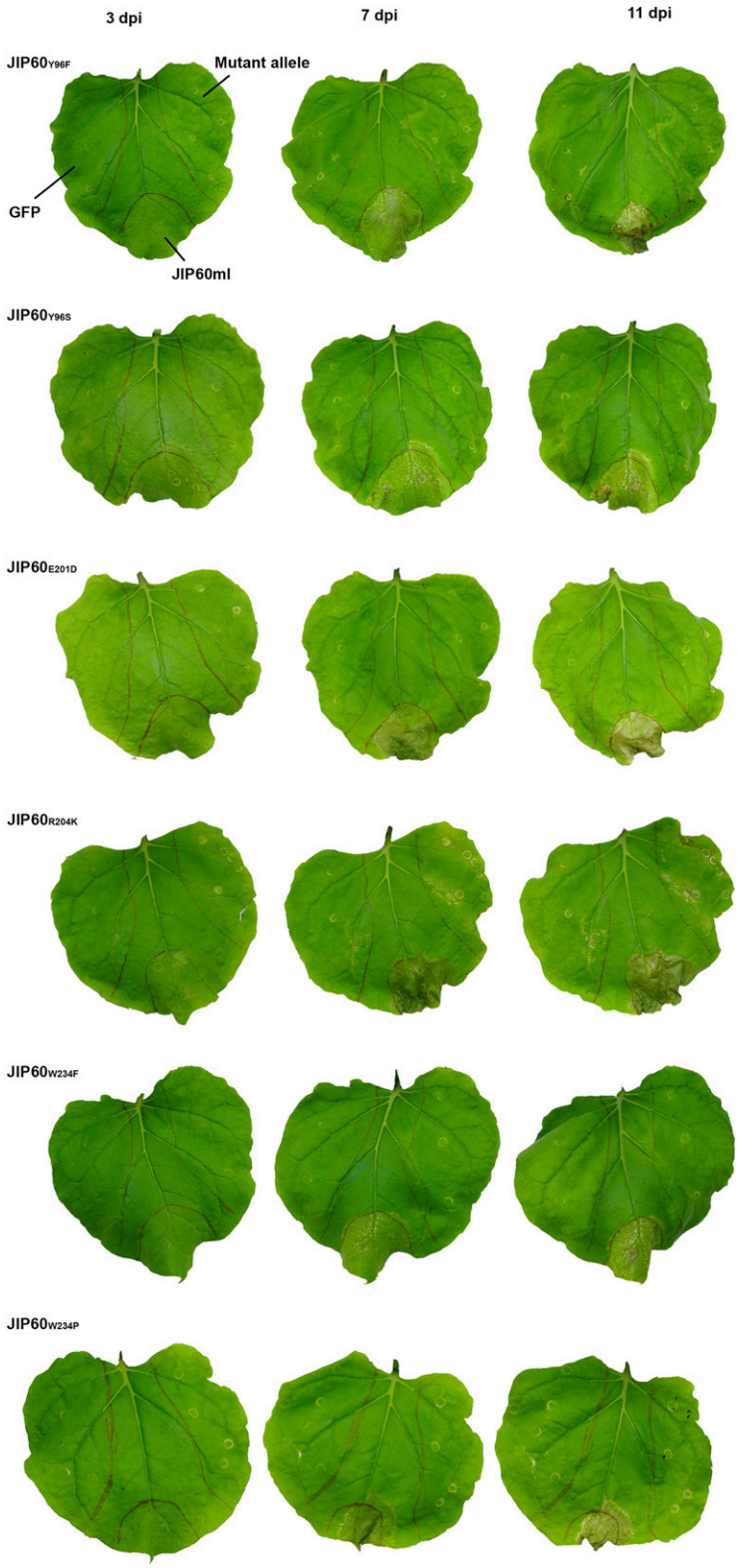

Figure 6. Time course of transient expression of isostructural or isofunctional JIP60 mutants in *N. benthamiana*. *Agrobacterium* strains carrying plasmids with JIP60 mutants were infiltrated into *N. benthamiana* (OD_{600} = 1.0) leaf zones as indicated by the marker outlines. JIP60ml-GFP or GFP-only were infiltrated as the positive and negative controls, respectively. Photographs were taken at 3, 7, and 11 dpi. The JIP60 mutants were obtained via site-directed mutagenesis of active-site residues substituted with either an isostructural or isofunctional amino acid. This experiment was repeated three times with similar outcomes.

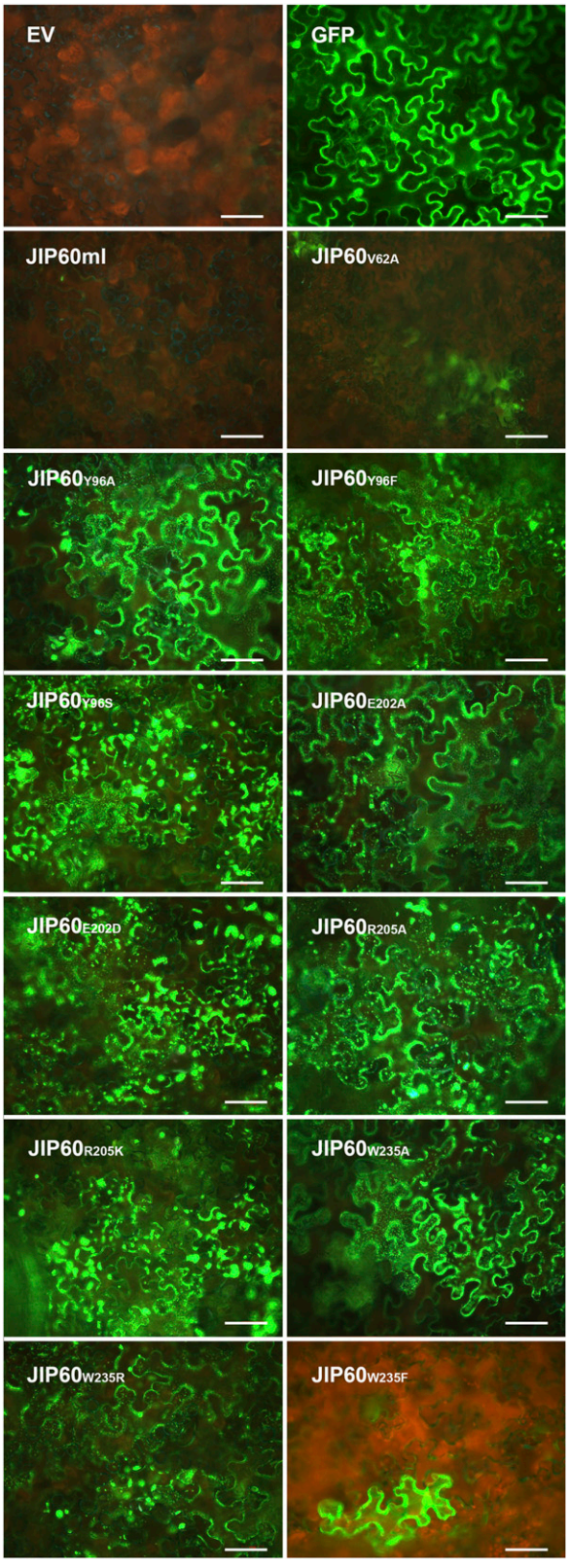

Figure 7. Micrographs of transiently expressed JIP60 variants in *N. benthamiana* observed by epifluorescence microscopy. *Agrobacterium* strains with plasmids encoding JIP60 variants conjugated to GFP were infiltrated into *N. bethamiana* (OD_{600} = 1.0). At 2 dpi, the samples were observed by epifluorescence microscopy and micrographs were taken. The excitation/emission filters used were those optimized for GFP imaging. All JIP60 variants, apart from JIP60ml, $JIP60_{V62A}$, and $JIP60_{W234F}$ show strong GFP signal, indicating successful expression. JIP60ml and the $JIP60_{V62A}$ are both functional variants, which is why little to no GFP was detected in these mutants. Scale bars = 200 μm.

activity on ribosomes in vitro using a wheat germ extract translation system. Templates for transcription of the JIP60ml variant genes were first created using PCR to add the T7 promoter upstream of the coding sequence. Then, the T7-JIP60ml variants were transcribed into mRNA with T7 RNA polymerase. Subsequently, mRNA encoding the JIP60ml variants was added to wheat germ extract alongside mRNA and incubated for 2 h at 25°C to achieve in vitro translation. Then luciferin was added to each sample and luminescence was measured to test the effect of cotranslating the JIP60ml variants and the luciferase mRNAs (Fig. 9).

The experiment was repeated three times and within each experiment five consecutive measurements were taken as technical repeats. To measure statistically the validity of the results, they were tested using a linear mixed model where the JIP60ml variants were treated as the fixed effect and the difference between experimental repetitions was considered the random effect. Subsequently, the significance between samples was assessed using Tukey's honestly significant difference (HSD) mean separation test to account for multiple testing. According to the linear mixed model, the difference between the repeats was responsible for ~49% of the variability between samples. The JIP60ml and JIP60V62A variants produced a consistent, statistically significant decrease in luciferase activity, with their respective medians at 1.2×10^5 fibrinolytic units (FU) and 0.7×10^5 FU, in comparison with the luciferase-only positive control (+ve) with its median of 1.9×10^5 FU (***$P < 0.001$ for both JIP60ml and $JIP60_{V62A}$, according to Tukey's HSD mean separation test). Addition of the $JIP60_{Y96F}$, $JIP60_{Y96S}$, $JIP60_{E201D}$, $JIP60_{R204K}$, and $JIP60_{W234F}$ variants resulted in no consistent decrease in luciferase activity: their medians did not vary significantly from that of the luciferase-only positive control, indicating loss of function. $JIP60_{W234P}$, which was predicted to have structural disruption due to Pro substitution, showed a statistically significant drop in luciferase activity (***$P < 0.001$, according to Tukey's HSD mean separation test), with a median of 1.7×10^5 FU. All conditions were statistically significant from the negative control (−ve), according to Tukey's HSD mean separation test.

A summary of the phenotypes observed following targeted mutagenesis is given in Supplemental Table S1.

DISCUSSION

JIP60ml Is a Potent Inducer of Cell Death

RIPs are a widespread group of proteins with a single catalytic function and are involved in diverse physiological processes, ranging from plant defense

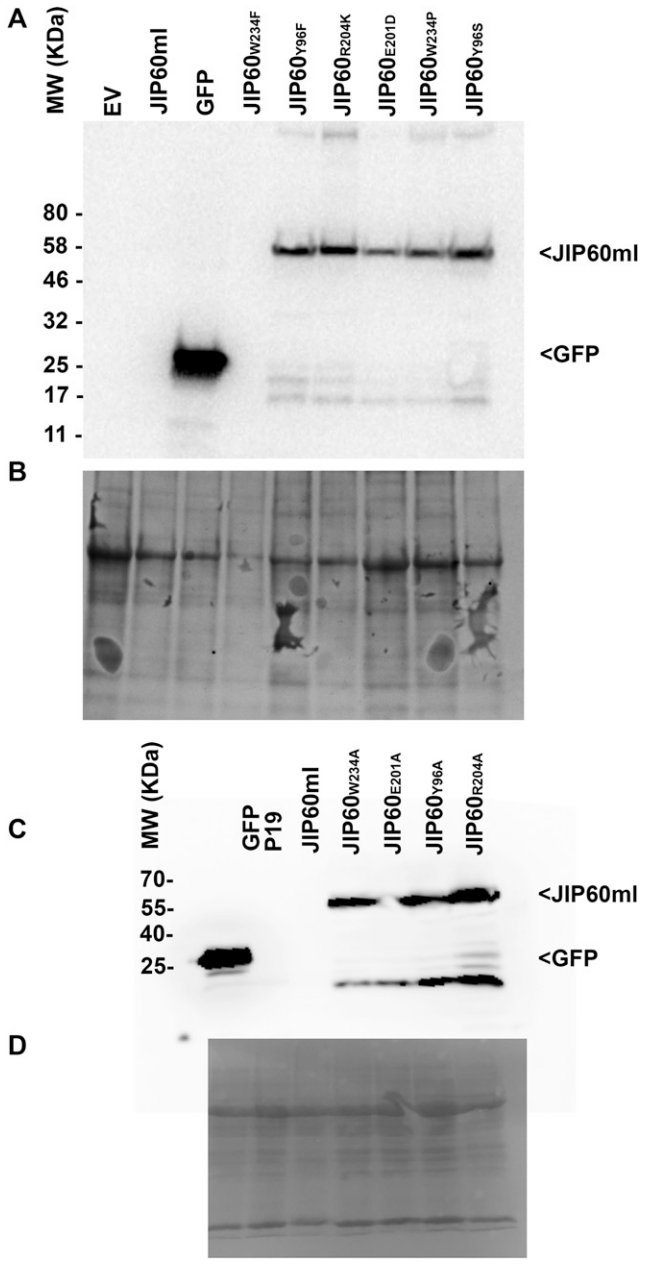

Figure 8. Western blots of protein extract from agroinfiltrated *N. bethamiana* leaves. *Agrobacterium* strains carrying JIP60ml variants (as indicated above the immunoblots) conjugated to GFP were infiltrated into *N. benthamiana* leaves (OD_{600} = 1.0). Agrobacteria containing an "empty vector" (EV) or GFP were used as negative and positive controls, respectively. At 3 dpi, leaf discs were collected and total proteins extracted and analyzed by western blotting using anti-GFP antibodies as the primary antibody. A and C, Western blots. To visualize the amount of total leaf proteins analyzed in the blots, the samples analyzed in A were separated by gel electrophoresis and stained with Coomassie Blue (B), and the samples analyzed in C were stained with Ponceau Red on the same membrane used for blotting (D).

against fungal, bacterial, and viral pathogens to translational regulation, senescence, and even amino acid storage (De Zaeytijd and Van Damme, 2017).

The barley RIP JIP60 is associated with senescence (Springer et al., 2015). In the case of JA-induced senescence, JIP60 accumulates and is associated with tissue necrosis. It is thought that the proteolytically processed, activated N-terminal domain of JIP60 inhibits translation at the elongation step which then triggers rapid cell death (Dunaeva and Goerschen, 1999). Here, we demonstrated that the presumptive catalytically active N-terminal domain of JIP60 is a potent trigger of cell death when expressed transiently in *N. benthamiana* leaves by *Agrobacterium*-mediated expression (agroinfiltration). These findings may explain that while full-length *JIP60* complementary DNA could be transformed stably into *N. benthamiana*, only the plants that were expressing JIP60 poorly were able to be regenerated and grown (Görschen et al., 1997). That is, high expression of JIP60 is likely to result in some production of an active JIP60 RIP, which could be highly toxic and kill the transgenic plants. In that study, the plants exhibited visible gene dose-dependent phenotypes such as severe stunting, premature senescence, and poor or no seed production. It is possible that some processing and activation of the full-length JIP60 occurred in planta.

This powerful cell suicide mechanism would be particularly effective at preventing infection by pathogenic organisms that depend on a living host cell for survival, for example, the obligate biotrophic powdery mildew fungi (Glawe, 2008). Consistent with this, these pathogenic fungi have evolved effector proteins that interfere with JIP60-mediated cell death by protecting the host ribosomes and inhibiting cell death (Pliego et al., 2013; Pennington et al., 2019).

The Mode of Action of JIP60

As observed in other plant RIPs, JIP60 possesses N-glycosidase activity and inhibits protein translation in vitro (Chaudhry et al., 1994; Dunaeva et al., 1999). However, the mode of action of JIP60 has not been described. In this work, we used HMMER and Phyre[2] to confirm that the amino acid sequence of the N-terminal domain of JIP60 displays a canonical ricin-like N-glycosidase fold with strong conservation of residues involved in catalysis. To infer how JIP60 works, we used targeted mutagenesis in the proposed catalytic residues and carried out functional analysis of the mutants in *N. benthamiana*.

Comparison of the predicted structures of JIP60 and JIP60ml shows only minimal changes in the orientation of side chains in key residues of the active site (Fig. 2C). It has been previously shown that removal of the 22-residue loop (amino acids 164–185 in the unprocessed protein) is required for full activation of the N-glycosidase activity of JIP60 (Chaudhry et al., 1994). It is still unclear whether this region alters the conformation of the active site to impair the catalytic activity of JIP60. An Asp-rich motif in this sequence (SSISGGIGNDDVDDDGNMLRAN) may directly interact with the catalytic site and block access to ligands or

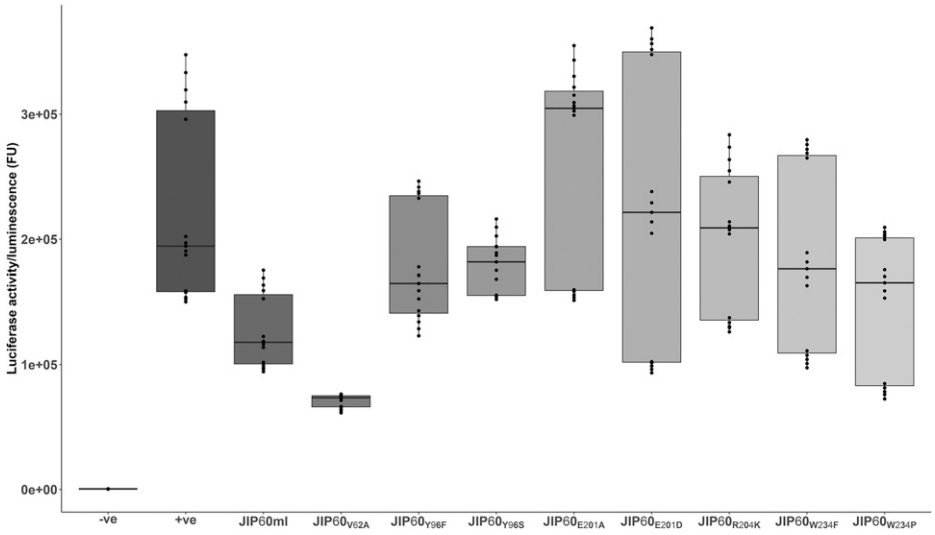

Figure 9. In vitro translation assay using JIP60ml variants in wheat germ extract. JIP60ml variants were transcribed into mRNA using T7 RNA polymerase. Subsequently, 1 μg of mRNA of each JIP60ml variant was added to wheat germ extract with 1 μg of luciferase mRNA, and the mixture was then incubated at 25°C for 2 h. The effect of JIP60ml variants on translation was measured indirectly by assaying the luciferase activity in each sample. JIP60ml and $JIP60_{V62A}$, which were functional in planta, led to a consistent and statistically significant drop in luciferase activity (***$P < 0.001$ for both JIP60ml and $JIP60_{V62A}$, according to Tukey's HSD mean separation test), with medians 1.2×10^5 FU and 0.7×10^5 FU, respectively. Interestingly, $JIP60_{W235P}$ showed a less defined, although statistically significant, decrease in luciferase activity (***$P < 0.001$, according to Tukey's HSD mean separation test), with median 1.7×10^5 FU. Other mutants, $JIP60_{Y96F}$, $JIP60_{Y96S}$, $JIP60_{E202D}$, $JIP60_{R205K}$, and $JIP60_{W235F}$, showed no statistically significant drop in luciferase activity, with their medians close to that of the positive control.

create an electrostatic repulsion toward its target RNA in the ribosome. Interestingly, this region aligns with comparable motifs in other proteins in the RIP family, e.g. in maize RIP: SYGDDCGSDEEEESGMLRAG (Uniprot K7USD0).

Similarly, using the crystal structure of maize RIP1 (Uniprot P25891), it has been argued that physical obstruction by the inactivation loop, and not conformational changes in the active site, prevents the RIP from interacting with ribosomes, thus making the protein inactive (Yang et al., 2010). We observed structural alignment of this region (EEEEVQMQMQMPEAADLAAAAAADPQAD) with the inactivation loop of JIP60.

Irrespective of how the inactivation loop works, we based the proposed reaction mechanisms on RNA depurination described for ricin (Wahome et al., 2011), which is the archetypal RIP for which the catalytic activity of the active site is fully understood. We hypothesized that E201 and R204 catalyze the cleavage of the glycosidic bond in the RNA substrate, while Y96 stabilizes the RNA in the active site. In order to test this model, we substituted Y96, E201, R204, and W234 with Ala, or residues with similar chemical or structural properties, and tested the effect of expressing these residues transiently in *N. benthamiana*; as a control, a change was made to a Val at position 62 (V62A) which was predicted not to affect the structure of the active site. In contrast to the wild type, JIP60ml, and the control mutant, none of the other JIP60ml mutants induced necrosis. We confirmed that the inactive mutants were expressed in the infiltrated leaves by visualization of the GFP tags by immunofluorescence microscopy and western blotting.

We were unable to detect intact JIP60ml protein from agroinfiltrated zones by western blotting, even before any symptoms of necrosis were visible. Consistent with this, there was no GFP signal in those zones. We interpret this to indicate that while JIP60ml protein is expressed by the plant, it is so active in inducing necrosis that the host cells producing it die before enough accumulates to levels at which it can be detected. This is not surprising, as RIPs tend to be extremely effective: a single ricin molecule is estimated to be sufficient to cause cell death when it reaches the intracellular target (Eiklid et al., 1980). Overall, our data support the view that JIP60ml catalytic activity proceeds in a way similar to that described for the "model RIP" ricin.

Interestingly, the JIP60-GFP conjugate loss-of-function mutants that can be detected by western blots also appear on fluorescent micrographs as scattered spots (puncta) in the cell cytosol; these puncta resemble processing bodies (also known as P-bodies; Eulalio et al., 2007; Luo et al., 2018). These observations suggest that the inactive JIP60ml variants aggregated and trafficked into cell processing bodies long enough to be detected.

The mutagenesis of the four candidate active-site residues (Y96, E201, R204, and W234), and the subsequent experiments, are consistent with the hypothesis that these residues are indeed part of the active site of the N-terminal domain of JIP60: they are all necessary for the RIP function of the protein, and any changes in these residues have very strong detrimental effects on

the function. The use of isofunctional and isostructural amino acids indicated that the RIP active site is very fragile, and even a small variation in a single residue, such as mutation from Glu to Asp, affected its functionality. This is also consistent with the high degree of conservation of these residues observed throughout RIP sequences in the databases. The reason why $JIP60_{W234F}$ did not show expression of GFP signal or protein levels on a western blot is unclear; it may indicate that this mutation determines instability of the construct in vivo.

Killing Activity In Planta Correlated with Inhibition of Protein Translation In Vitro

Using a commercial assay that employs luciferase as a reporter system, we subsequently investigated the action of JIP60ml and JIP60ml mutants on protein translation in vitro to test whether there was any correlation between the cell-death-inducing activity of the recombinant proteins and their capacity to interfere with ribosome activity. In general, we observed large variations in the overall output between experiments; we therefore chose to use the "luciferase only" positive control as a reference sample in each experiment. As expected, the JIP60ml and the $JIP60_{V62A}$ mutant significantly decreased the overall translation activity, even though they never entirely abolished it.

In the case of the $JIP60_{W234P}$ mutant, in planta expression did not cause any visible necrosis, whereas in vitro translation caused a statistically significant inhibition of luciferase translation. This suggests that the $JIP60_{W234P}$ mutant may have retained at least part of its function. Pro residues tend to create a kink within molecular structures, often leading to misfolding of the protein if introduced as a mutation (Yaron et al., 1993). This may have been sufficient to determine the instability in the protein that led to the inability to detect it in the plant when transiently expressed.

CONCLUSIONS

Overall, our results demonstrated that the N-terminal domain of JIP60 is a RIP and that transient expression of an activated fragment was a potent inducer of cell death in planta. The predicted conserved residues of RIPs (Y96, E201, R204, and W234) were necessary for the function of the protein, in analogy to the action of the RIP ricin, and we consider that the mode of catalytic action illustrated in Figure 3 is validated. Interference with any of these residues resulted in loss of function in vivo and in vitro, confirming their role in the active site of JIP60. In the future, a functional validation of the role played by barley JIP60 and its paralogs in plant immunity, and how certain fungi may target them with effector proteins, may be desirable. This could be achieved by targeted mutation of the genes using, for example, clustered regularly interspaced short palindromic repeats (CRISPR)/CRISPR-associated protein 9 (Cas9) genome editing techniques.

MATERIALS AND METHODS

Nicotiana benthamiana

N. benthamiana plants were grown in a chamber under long-day conditions (16-h-light, 8-h-dark) at 24°C during the day and 19°C at night. Initially, *N. benthamiana* seeds were grown in sphagnum moss peat compost (Levington Advance F2+S) with 30% vermiculite (Sinclair Pro) in a single pot under transparent cover to create a high humidity condition. One-week-old seedlings were then transferred to individual square 10-cm pots and grown for 3 weeks.

Bioinformatics

The RIP domain analysis was performed using HMMER (phmmer version 3.2.1; http://hmmer.org/) against EnsemblPlant database. The consensus of the RIP amino acid sequence was obtained using JalView (https://www.jalview.org/) by aligning the RIP family sequences (PF00161) using the neighbor joining tree BLOSUM62 algorithm (Eddy, 2004). The conserved amino acids were highlighted using the Clustal (Larkin et al., 2007) color scheme convention. The prediction of JIP60 and JIP60ml protein fold was performed using the Phyre^2 algorithm, using the "intense" setting (Kelley et al., 2015). Phyre^2 yielded homology models for these constructs with >90% accuracy.

JIP60ml Construct

In this study, a recombinant JIP60ml construct was used in the in planta coagroinfiltration system. The JIP60 gene from genomic DNA of barley (*Hordeum vulgare*; GenBank sequence ID: KY929371.1) was cloned into the pDONR201 plasmid (GATEWAY entry plasmid). JIP60ml was created by cloning the first 287 amino acids of JIP60 (corresponding to the N-terminal RIP domain, GenPept sequence ID: AVK42932.1) and then excising the sequence corresponding to protein residues 163–185, i.e. the inactivation loop of JIP60, and replacing them with a Met-Leu linker (note that the Met-Leu already exists in wild-type JIP60; see Supplemental Fig. S2). Subsequently, for agroinfiltration experiments, JIP60ml was cloned onto the pK7FWG2 backbone, which is an *Agrobacterium* compatible vector in which GFP is fused to the C-terminal of an inserted gene.

Agroinfiltrations of *N. benthamiana*

Agrobacterium tumefaciens strain GV3101 (resistant to rifampicin carrying a helper plasmid conferring gentamycin resistance) carrying required plasmid constructs were maintained on lysogeny broth (LB) agar (1% [w/v] tryptone, 0.05% [w/v] yeast extract, 1% [w/v] NaCl, and 1.5% [w/v] agar) in petri dishes (90 × 15 mm) with the appropriate antibiotics at a concentration of 50 μg mL^{-1} for kanamycin and 100 μg mL^{-1} for spectinomycin and grown at 28°C for up to 2 d. Afterward, the bacteria were collected by scooping the cells with a sterile loop into a 1.5-mL tube, washed twice by resuspending in 1 mL of sterile water, centrifuged at 14,000*g* for 1 min, removing the supernatant by aspiration and repeating the procedure. The pellets were then suspended in 1 mL of MMA buffer (10 mM MES [pH 5.7], 10 mM $MgCl_2$) and the optical density at 600 nm (OD_{600}) was measured. Finally, the Agrobacteria suspensions were diluted to OD_{600} = 1.0 with an appropriate amount of MMA buffer and mixed thoroughly prior to infiltrations. *N. benthamiana* plants (~4 weeks old) were used for agroinfiltrations.

In order to ensure stronger and more consistent transient expression of the transgene, *Agrobacterium* containing a plasmid encoding the P19 protein (OD_{600} = 0.1) was coinfiltrated in all experiments. P19 is a viral suppressor of gene silencing from *Tomato bush stunt virus* (*TBSV*; Voinnet et al., 2003).

Transformation of Chemically Competent *Escherichia coli*

All transformations of *E. coli* (DH5α) in this study were performed on chemically competent bacteria prepared using the calcium chloride method (Swords, 2003). Initially, a 25-μL aliquot of cell suspension was inoculated with

100 ng of the required plasmid and was incubated on ice for 30 min. Afterward, the bacteria were heat shocked at 42°C for 30 to 45 s and then placed on ice for 2 min before addition of 150 μL of LB medium and incubation at 37°C for 1 h. Finally, the bacteria were plated on LB agar plates with the appropriate antibiotic for selection and grown at 37°C until distinct colonies were visible.

Electroporation of Electro-Competent *Agrobacterium*

Electro-competent *Agrobacterium* was prepared as described (Wise et al., 2006). Subsequently, 50-μL aliquots were inoculated with 100 ng of the desired plasmid and electroporated at 2.2 kV for 5.9 ms with MicroPulser (BioRad) using the *Agrobacterium*-specific program. The bacteria were placed on ice for 15 min before 250 μL of LB medium were added and the bacteria were incubated at 28°C with shaking at 220 rpm for 1 h. The *Agrobacterium* cells were then plated on appropriate selective LB agar.

Site-Directed Mutagenesis of JIP60ml

The list of targeted mutations to JIP60ml is given in Supplemental Table S1. Primers were designed to mutagenize the JIP60ml sequence in the entry vector pDONR201 using the QuikChange I protocol for JIP60ml$_{Y96A}$ and QuikChange II protocol for the remaining mutations. The primers are listed in Supplemental Table S2.

QuikChange I mutagenesis was performed by first amplifying the JIP60ml clone in a thermocycler with *Pfu* high fidelity polymerase (Promega) using the following conditions: 2 min at 95°C, then 18 cycles of 30 s at 95°C, 30 s at 52°C, and 7 min 30 s at 72°C, ending with 20 min at 72°C. The template was then digested by adding *Dpn*I restriction enzyme (New England Biolabs) directly to the PCR mix at 37°C for 3 h and the product was ligated with T4 ligase (Promega) at 25°C overnight. The ligated product was then transformed into chemically competent *E. coli*. Selected colonies were mini-prepped and sequenced by GATC Biotech to confirm successful mutagenesis.

QuikChange II mutagenesis was performed by amplifying the JIP60ml sequence in a thermocycler under the same conditions as for QuikChange I. The template was digested with *Dpn*I restriction enzyme (New England Biolabs) at 37°C for 3 h and then the product was directly transformed into chemically competent *E. coli*. The colonies were sequenced to confirm successful mutagenesis.

Microscopy

Plant leaf discs were placed onto microscope slides and visualized using an Axioplan 2 light/fluorescence microscope with a filter setup optimized for detection of GFP fluorescence. Micrographs were captured using AxioVision control (version 3.1).

Protein Extraction from Plants

About 150 mg of plant material (up to eight 10 mm diameter leaf disks), were ground in liquid nitrogen to fine powder with a mortar and pestle and then collected in a 1.5 ml centrifuge tube. Protein extraction buffer (150 μL), either native (0.01% [v/v] Tween 20, 50 mM sodium phosphate [pH 8], 300 mM NaCl, 1 mM $MgCl_2$, 1% [w/v] PVPP) or denaturing (7 M Urea, 2 M Thiourea, 10 mM DTT, 0.1% [w/v] CHAPS, 1x cOmplete mini protease inhibitor (EDTA-free; Roche). was added along with 425–600 μm glass beads (Sigma Aldrich; catalog No. G8772). The tube was mixed with a vortex for 10 s, the contents were allowed to settle on ice for 7 min, and then mixed with a vortex again for 10 s Subsequently, the tube was centrifuged at 4°C at 20,800 rcf for 30 min. The supernatant was carefully transferred into a fresh, prechilled 1.5 ml centrifuge tube, and then centrifuged again at 4°C at 20,800*g* for 30 min. The resulting supernatant constituted the protein extract.

SDS PAGE

SDS-Polyacrylamide gels (5% stacking gel: 0.1% [w/v] SDS, 125 mM Tris-HCl [pH 6.8], 16% [v/v] 37.5:1 acrylamide/bis-acrylamide 30% solution, 0.1% [w/v] ammonium persulfate, and 0.1% [v/v] TEMED [*N*,*N*,*N*′,*N*′-tetramethylethylenediamine]; 12% separating gel: 0.1% [w/v] SDS, 400 mM Tris-HCl [pH 8.8], 40% [v/v] polyacrylamide 30% solution, 0.1% [w/v] ammonium persulfate, and 0.04% [v/v] TEMED) were cast using a Mini-PROTEAN Tetra Vertical Handcast system (Bio-Rad). The protein samples were mixed with 4× loading buffer (200 mM Tris-Cl [pH 6.8], 8% [w/v] SDS, 0.04% [w/v] bromophenol blue, 40% [v/v] glycerol, and 2% [v/v] β-mercaptoethanol), denatured at 95°C for 10 min, and subsequently loaded on the gel. The gels were resolved using the Mini-PROTEAN Tetra Vertical system (Bio-Rad) at 100 V for ~90 min in 1× running buffer (25 mM Tris-HCl, 250 mM Gly, and 0.1% SDS). Gels were stained with colloidal Coomassie Blue staining (Candiano et al., 2004).

Western Blotting

Protein transfers onto a polyvinylidene fluoride membrane (Amersham) were performed in a Mini TransBlot cell (Bio-Rad) at 100 V for 60 min in a 1× transfer buffer (50 mM Tris-HCl, 400 mM Gly, and 20% [v/v] methanol). Subsequently, the membrane was incubated in 5% [w/v] dry milk in Tris-buffered saline with Tween 20 (TBST; 50 mM Tris-HCl [pH 7.6], 150 mM NaCl, and 0.1% [v/v] Tween 20), shaking for 60 min at room temperature. Then the membrane was incubated in 5% [w/v] dry skimmed milk in TBST with the primary antibody (rabbit anti-GFP IgG; Thermo Fisher Scientific) at a 1:10,000 dilution with overnight shaking at 4°C. The membrane was then washed four times with TBST, shaken at room temperature for 10 min, and then incubated with secondary antibody (goat antirabbit IgG; Invitrogen) at a dilution of 1:3,000 in 5% (w/v) dry skimmed milk in TBST at room temperature for 60 min. The membrane was then washed again four times with TBST at room temperature, shaking, for 10 min. The detection was performed using SuperSignal West Dura Substrate (ThermoFisher) according to the manufacturer's description. The chemiluminescence was visualized using a LAS-3000 imager (FujiFilm).

In Vitro Transcription/Translation Assay

The in vitro transcription/translation assays were performed using a TnT Coupled Reticulocyte Lysate System (catalog no. L4610, Promega). The constructs for the study were amplified as linear PCR products with GoTaq polymerase (Promega) with 5% dimethyl sulfoxide using the following conditions: 95°C for 2 min, 35 cycles of 30 s at 95°C, 30 s at 50°C, and 90 s at 72°C, finishing with 5 min at 72°C. The 5 μL reactions were incubated at 30°C for 90 min. The "forward" DNA primers included a T7 promoter attached to the 5′ end of the gene-specific sequence (Supplemental Table S2). Subsequently, the 5 μL of the reactions were added to 50 μL of Luciferase Assay Reagent (catalog no. E1500, Promega) in a flat-bottom 96-well black plate and the luminescence was immediately measured with a Tecan illuminometer. Five consecutive measurements were taken with 1,000 ms attenuation, with 10 s between measurements.

Statistical Analysis

All statistical analysis was performed using R scripting language (R Core Team 2013). The results were analyzed first using a Linear Mixed model, then with a Tukey's HSD mean separation test. The experiments were repeated three times, independently (on three separate days), and each data point was the result of five technical replicates.

Accession Numbers

Sequence data from this article can be found in the GenBank/EMBL data libraries under accession numbers Q00531 (JIP60 [60 kD JA-induced protein; UniProtKB]).

Supplemental Data

The following supplemental materials are available.

Supplemental Table S1. List of JIP60ml mutations and their properties.

Supplemental Table S2. List of primers used in mutagenesis of JIP60.

Supplemental Figure S1. The cell death-inducing activity of JIP60ml is highly potent.

Supplemental Figure S2. Alignment of JIP60 and JIP60ml to illustrate the modifications carried out to obtain the active N-terminal domain of JIP60.

Received August 27, 2019; accepted February 7, 2020; published March 2, 2020.

LITERATURE CITED

Andresen I, Becker W, Schlüter K, Burges J, Parthier B, Apel K (1992) The identification of leaf thionin as one of the main jasmonate-induced proteins of barley (*Hordeum vulgare*). Plant Mol Biol **19:** 193–204

Bachmann A, Hause B, Maucher H, Garbe E, Vörös K, Weichert H, Wasternack C, Feussner I (2002) Jasmonate-induced lipid peroxidation in barley leaves initiated by distinct 13-LOX forms of chloroplasts. Biol Chem **383:** 1645–1657

Barbieri L, Ferreras JM, Barraco A, Ricci P, Stirpe F (1992) Some ribosome-inactivating proteins depurinate ribosomal RNA at multiple sites. Biochem J **286:** 1–4

Bieri S, Potrykus I, Fütterer J (2003) Effects of combined expression of antifungal barley seed proteins in transgenic wheat on powdery mildew infection. Mol Breed **11:** 37–48

Bohlmann H, Clausen S, Behnke S, Giese H, Hiller C, Reimann-Philipp U, Schrader G, Barkholt V, Apel K (1988) Leaf-specific thionins of barley—A novel class of cell wall proteins toxic to plant-pathogenic fungi and possibly involved in the defence mechanism of plants. EMBO J **7:** 1559–1565

Bolognesi A, Bortolotti M, Maiello S, Battelli MG, Polito L (2016) Ribosome-inactivating proteins from plants: A historical overview. Molecules **21:** 1627

Candiano G, Bruschi M, Musante L, Santucci L, Ghiggeri GM, Carnemolla B, Orecchia P, Zardi L, Righetti PG (2004) Blue silver: A very sensitive colloidal Coomassie G-250 staining for proteome analysis. Electrophoresis **25:** 1327–1333

Chaudhry B, Müller-Uri F, Cameron-Mills V, Gough S, Simpson D, Skriver K, Mundy J (1994) The barley 60 kDa jasmonate-induced protein (JIP60) is a novel ribosome-inactivating protein. Plant J **6:** 815–824

Chini A, Gimenez-Ibanez S, Goossens A, Solano R (2016) Redundancy and specificity in jasmonate signalling. Curr Opin Plant Biol **33:** 147–156

Cunningham BC, Wells JA (1989) High-resolution epitope mapping of hGH-receptor interactions by alanine-scanning mutagenesis. Science **244:** 1081–1085

De Zaeytijd J, Van Damme EJ (2017) Extensive evolution of cereal ribosome-inactivating proteins translates into unique structural features, activation mechanisms, and physiological roles. Toxins (Basel) **9:** 123

Di R, Tumer NE (2015) Pokeweed antiviral protein: Its cytotoxicity mechanism and applications in plant disease resistance. Toxins (Basel) **7:** 755–772

Duan Z, Lv G, Shen C, Li Q, Qin Z, Niu J (2014) The role of jasmonic acid signalling in wheat (*Triticum aestivum* L.) powdery mildew resistance reaction. Eur J Plant Pathol **140:** 169–183

Dunaeva M, Goebel C, Wasternack C, Parthier B, Goerschen E (1999) The jasmonate-induced 60 kDa protein of barley exhibits *N*-glycosidase activity in vivo. FEBS Lett **452:** 263–266

Dunaeva M, Goerschen E (1999) RIP-JIP60 alters conformation of ribosomes *in vivo*. Biochem Biophys Res Commun **258:** 572–573

Eddy SR (2004) Where did the BLOSUM62 alignment score matrix come from? Nat Biotechnol **22:** 1035–1036

Eiklid K, Olsnes S, Pihl A (1980) Entry of lethal doses of abrin, ricin and modeccin into the cytosol of HeLa cells. Exp Cell Res **126:** 321–326

Endo Y, Tsurugi K (1987) RNA N-glycosidase activity of ricin A-chain. Mechanism of action of the toxic lectin ricin on eukaryotic ribosomes. J Biol Chem **262:** 8128–8130

Eulalio A, Behm-Ansmant I, Izaurralde E (2007) P bodies: At the crossroads of post-transcriptional pathways. Nat Rev Mol Cell Biol **8:** 9–22

Finn RD, Clements J, Arndt W, Miller BL, Wheeler TJ, Schreiber F, Bateman A, Eddy SR (2015) HMMER web server: 2015 update. Nucleic Acids Res **43**(W1): W30–W38

Fonseca S, Chini A, Hamberg M, Adie B, Porzel A, Kramell R, Miersch O, Wasternack C, Solano R (2009) (+)-7-*iso*-Jasmonoyl-L-isoleucine is the endogenous bioactive jasmonate. Nat Chem Biol **5:** 344–350

Glawe DA (2008) The powdery mildews: A review of the world's most familiar (yet poorly known) plant pathogens. Annu Rev Phytopathol **46:** 27–51

Goossens J, Fernández-Calvo P, Schweizer F, Goossens A (2016) Jasmonates: Signal transduction components and their roles in environmental stress responses. Plant Mol Biol **91:** 673–689

Görschen E, Dunaeva M, Hause B, Reeh I, Wasternack C, Parthier B (1997) Expression of the ribosome-inactivating protein JIP60 from barely in transgenic tobacco leads to an abnormal phenotype and alterations on the level of translation. Planta **202:** 470–478

Hause B, Hertel SC, Klaus D, Wasternack C (1999) Cultivar-specific expression of the jasmonate-induced protein of 23 kDa (JIP-23) occurs in *Hordeum vulgare* L. by jasmonates but not during seed germination. Plant Biol **1:** 83–89

Hause B, Zurnieden U, Lehmann J, Wasternack C, Parthier B (1994) Intracellular localization of jasmonate-induced proteins in barley leaves. Bot Acta **107:** 333–341

Hudak KA, Dinman JD, Tumer NE (1999) Pokeweed antiviral protein accesses ribosomes by binding to L3. J Biol Chem **274:** 3859–3864

Kelley LA, Mezulis S, Yates CM, Wass MN, Sternberg MJE (2015) The Phyre^2 web portal for protein modeling, prediction and analysis. Nat Protoc **10:** 845–858

Krivdova G, Neller KCM, Parikh BA, Hudak KA (2014) Antiviral and antifungal properties of RIPs. In F Stirpe, and DA Lappi, eds, Ribosome-Inactivating Proteins. John Wiley & Sons, Oxford, pp 198–211

Lancaster L, Lambert NJ, Maklan EJ, Horan LH, Noller HF (2008) The sarcin-ricin loop of 23S rRNA is essential for assembly of the functional core of the 50S ribosomal subunit. RNA **14:** 1999–2012

Larkin MA, Blackshields G, Brown NP, Chenna R, McGettigan PA, McWilliam H, Valentin F, Wallace IM, Wilm A, Lopez R, et al (2007) Clustal W and Clustal X version 2.0. Bioinformatics **23:** 2947–2948

Leah R, Tommerup H, Svendsen I, Mundy J (1991) Biochemical and molecular characterization of three barley seed proteins with antifungal properties. J Biol Chem **266:** 1564–1573

Lee BG, Kim MK, Kim BW, Suh SW, Song HK (2012) Structures of the ribosome-inactivating protein from barley seeds reveal a unique activation mechanism. Acta Crystallogr D Biol Crystallogr **68:** 1488–1500

Lee MW, Yang Y (2006) Transient expression assay by agroinfiltration of leaves. In J Salinas, and JJ Sanchez-Serrano, eds, Arabidopsis Protocols, Methods in Molecular Biology 323. Humana Press, Totowa, NJ, pp 225–230

Leopold J, Hause B, Lehmann J, Graner A, Parthier B, Wasternack C (1996) Isolation, characterization and expression of a cDNA coding for a jasmonate-inducible protein of 37 kDa in barley leaves. Plant Cell Environ **19:** 675–684

Lin JY, Tserng KY, Chen CC, Lin LT, Tung TC (1970) Abrin and ricin: new anti-tumour substances. Nature **227:** 292–293

Luo Y, Na Z, Slavoff SA (2018) P-Bodies: Composition, properties, and functions. Biochemistry **57:** 2424–2431

Madeira F, Park YM, Lee J, Buso N, Gur T, Madhusoodanan N, Basutkar P, Tivey ARN, Potter SC, Finn RD, et al (2019) The EMBL-EBI search and sequence analysis tools APIs in 2019. Nucleic Acids Res **47**(W1): W636–W641

Maucher H, Hause B, Feussner I, Ziegler J, Wasternack C (2000) Allene oxide synthases of barley (*Hordeum vulgare* cv. Salome): Tissue specific regulation in seedling development. Plant J **21:** 199–213

Maucher H, Stenzel I, Miersch O, Stein N, Prasad M, Zierold U, Schweizer P, Dorer C, Hause B, Wasternack C (2004) The allene oxide cyclase of barley (*Hordeum vulgare* L.)—Cloning and organ-specific expression. Phytochemistry **65:** 801–811

Morrison KL, Weiss GA (2001) Combinatorial alanine-scanning. Curr Opin Chem Biol **5:** 302–307

Narayanan S, Surendranath K, Bora N, Surolia A, Karande AA (2005) Ribosome inactivating proteins and apoptosis. FEBS Lett **579:** 1324–1331

Nielsen K, Boston RS (2001) Ribosome-inactivating proteins: A plant perspective. Annu Rev Plant Physiol Plant Mol Biol **52:** 785–816

Pastan I, Chaudhary V, FitzGerald DJ (1992) Recombinant toxins as novel therapeutic agents. Annu Rev Biochem **61:** 331–354

Pennington HG, Jones R, Kwon S, Bonciani G, Thieron H, Chandler T, Luong P, Morgan SN, Przydacz M, Bozkurt T, et al (2019) The fungal ribonuclease-like effector protein CSEP0064/BEC1054 represses plant immunity and interferes with degradation of host ribosomal RNA. PLoS Pathog **15:** e1007620

Pliego C, Nowara D, Bonciani G, Gheorghe D, Xu R, Surana P, Whigham E, Nettleton D, Bogdanove AJ, Wise R, et al (2013) Host-induced gene silencing in barley powdery mildew reveals a class of ribonuclease-like effectors. Mol Plant Microbe Interact **26:** 633–642

Reinbothe C, Parthier B, Reinbothe S (1997) Temporal pattern of jasmonate-induced alterations in gene expression of barley leaves. Planta **201:** 281–287

Reinbothe S, Reinbothe C, Lehmann J, Becker W, Apel K, Parthier B (1994) JIP60, a methyl jasmonate-induced ribosome-inactivating protein involved in plant stress reactions. Proc Natl Acad Sci USA **91:** 7012–7016

Repka V, Fischerova I, Silharova K (2001) Methyl jasmonate induces a hypersensitive-like response of grapevine in the absence of avirulent pathogens. Vitis **40:** 5–10

Rustgi S, Pollmann S, Buhr F, Springer A, Reinbothe C, von Wettstein D, Reinbothe S (2014) JIP60-mediated, jasmonate- and senescence-induced molecular switch in translation toward stress and defense protein synthesis. Proc Natl Acad Sci USA **111:** 14181–14186

Schrot J, Weng A, Melzig MF (2015) Ribosome-inactivating and related proteins. Toxins (Basel) **7:** 1556–1615

Schuster-Böckler B, Schultz J, Rahmann S (2004) HMM Logos for visualization of protein families. BMC Bioinformatics **5:** 7

Springer A, Acker G, Bartsch S, Bauerschmitt H, Reinbothe S, Reinbothe C (2015) Differences in gene expression between natural and artificially induced leaf senescence in barley. J Plant Physiol **176:** 180–191

Staswick PE, Tiryaki I (2004) The oxylipin signal jasmonic acid is activated by an enzyme that conjugates it to isoleucine in Arabidopsis. Plant Cell **16:** 2117–2127

Stirpe F (2013) Ribosome-inactivating proteins: From toxins to useful proteins. Toxicon **67:** 12–16

Stirpe F, Barbieri L, Battelli MG, Soria M, Lappi DA (1992) Ribosome-inactivating proteins from plants: Present status and future prospects. Biotechnology (N Y) **10:** 405–412

Swords WE (2003) Chemical transformation of *E. coli*. In N Casali, and A Preston, eds, *E coli* Plasmid Vectors: Methods and Applications, Methods in Molecular Biology 235. Humana Press, Totowa, NJ, pp 49–54

Vigers AJ, Roberts WK, Selitrennikoff CP (1991) A new family of plant antifungal proteins. Mol Plant Microbe Interact **4:** 315–323

Voinnet O, Rivas S, Mestre P, Baulcombe D (2003) An enhanced transient expression system in plants based on suppression of gene silencing by the p19 protein of tomato bushy stunt virus. Plant J **33:** 949–956

Vörös K, Feussner I, Kühn H, Lee J, Graner A, Löbler M, Parthier B, Wasternack C (1998) Characterization of a methyljasmonate-inducible lipoxygenase from barley (*Hordeum vulgare* cv. Salome) leaves. Eur J Biochem **251:** 36–44

Wahome PG, Robertus JD, Mantis NJ (2011) Small-molecule inhibitors of ricin and Shiga toxins. In N Mantis, ed, Ricin and Shiga Toxins: Pathogenesis, Immunity, Vaccines and Therapeutics, Current Topics in Microbiology and Immunology 357. Springer, New York, pp 179–207

Wasternack C, Feussner I (2018) The oxylipin pathways: Biochemistry and function. Annu Rev Plant Biol **69:** 363–386

Wasternack C, Hause B (2013) Jasmonates: Biosynthesis, perception, signal transduction and action in plant stress response, growth and development. An update to the 2007 review in Annals of Botany. Ann Bot **111:** 1021–1058

Wasternack C, Strnad M (2018) Jasmonates: News on occurrence, biosynthesis, metabolism and action of an ancient group of signaling compounds. Int J Mol Sci **19:** 2539

Wise AA, Liu Z, Binns AN (2006) Three methods for the introduction of foreign DNA into *Agrobacterium*. In K Wang, ed, Agrobacterium Protocols, Methods in Molecular Biology 1223. Humana Press, Totowa, NJ, pp 43–54

Yang Y, Mak AN-S, Shaw P-C, Sze KH (2010) Solution structure of an active mutant of maize ribosome-inactivating protein (MOD) and its interaction with the ribosomal stalk protein P2. J Mol Biol **395:** 897–907

Yaron A, Naider F, Scharpe S (1993) Proline-dependent structural and biological properties of peptides and proteins. Crit Rev Biochem Mol Biol **28:** 31–81